Journal of the European Ceramic Society 18 (1998) 725–733

PII: S0955-2219(97)00177-5
0955-2219/98/$19.00 + 0.00

Correlation between Microstructure and Electrical Properties of SiC-based Fibres Derived from Organosilicon Precursors

G. Chollon,[a]* R. Pailler,[a] R. Canet[b] and P. Delhaes[b]

[a]Laboratoire des composites Thermostructuraux, UMR 47 (CNRS-SEP-UB1), 3, allée de La Boétie, 33600 Pessac, France
[b]Centre de Recherche Paul Pascal, CNRS, UPR-8641, Avenue A. Schweitzer, 33600 Pessac, France

(Received 17 March 1997; accepted 26 September 1997)

Abstract

The chemical, structural and electrical properties of various SiC-based fibres prepared from the pyrolysis of organosilicon precursors were studied as a function of their maximum (post)processing temperature T_p. *The magnitude of the electrical conductivity* (σ) *and its thermal dependence (the apparent activation energy* E_a) *are mainly controlled by the carbon excess present in the fibres. The free carbon phase is observed by TEM analysis as turbostratic stacks of aromatic carbon layers. The extent of those carbon domains (in length:* L_a *and thickness:* N) *increases with* T_p. *The amount of free carbon but above all its microstructure (i.e. the size of the carbon domains and their residual hydrogen content) and its microtexture (isolated domains or interconnected network) govern the electrical properties of the fibres through a percolation effect.* © *1998 Elsevier Science Limited. All rights reserved*

1 Introduction

Silicon carbide fibres are one of the most promising refractory reinforcements for CMC's for high temperature uses in oxidizing atmospheres. Because of the strength of the Si-C covalent bond, silicon carbide combines excellent fracture strength, stiffness and creep resistance up to 1500°C. Furthermore it has an excellent oxidation resistance, owing to the formation of a protective silica layer. SiC fibres have been first prepared by chemical vapor deposition (CVD). However, these fibres are too large in diameter (100–150 mm) to be weavable and their high manufacturing cost precludes volume applications. In 1975 a breakthrough in the SiC fibres production technology was achieved by S. Yajima *et al.*[1,2] Their approach to prepare small diameter continuous SiC fibres involved a route close to the processing of carbon fibres. These fibres are now sold under the trade name Nicalon (by Nippon Carbon Co. Ltd, Yokohama 221, Japan) and are extensively used for reinforcing polymers, metals, glass and ceramic composites. Since 1975, a lot of different sorts of fibres have been produced according to processes derived from the Yajima route. The processing of the fibres generally involves three steps: (1) the spinning of the organosilicon precursor (e.g. a polycarbosilane PCS) in the molten state, (2) a chemical or a physical curing treatment to make the polymer fibres infusible and (3) the pyrolysis of the cured-filaments in an inert atmosphere yielding the final SiC-based ceramic fibres.[1,2] By using various polymer precursors, curing treatments and pyrolysis conditions, various types of fibres with specific properties have been prepared and some of them have been commercialized. Electronic and magnetic properties provide valuable information for a better understanding of the structure of nanocrystalline ceramics, especially in the case of free-carbon containing materials like most of the polymer-based SiC fibres. Furthermore, these properties are of interest for technologies for the control of the radar signature of composite structures. The aim of this paper is to investigate the influence of the processing routes and eventually of subsequent thermal treatments of such fibres on their electrical and magnetic behaviour, together with their chemical and structural properties.

*To whom correspondence should be addressed. Now at National Institute of Materials and Chemical Research, 1-1 Higashi, Tsukuba, Ibaraki 305, Japan.

2 Experimental

2.1 Description of the fibres

2.1.1 Nicalon NL 200 from Nippon Carbon
This commercial fibre is the most widely used SiC-based reinforcement in composites for industrial applications. The polymeric precursor used is a PCS of general formula —(–CH_2–$SiHCH_3$–)— and the curing process is a simple oxidation in air. This fibre has been widely studied.[3–9] It consists of nanometric SiC crystals (~2 nm), carbon clusters (~15 at% of free carbon) and an amorphous silicon oxycarbide phase SiO_xC_y, the oxygen (~13 at%) being introduced during the curing process.[3–6] The Nicalon NL 200 has a limited thermal stability. The SiO_xC_y phase decomposes above 1100–1200°C into CO and SiO leading to a strong decrease-of strength.[6–9] It has been shown that the thermal stability of polymer-derived fibres can be improved by reducing their oxygen content and therefore, by using an oxygen-free curing process.[10–15]

Except the Nicalon NL 200 which is the reference material, all the fibres studied and described below are prepared according to a physical oxygen-free curing process.

2.1.2 Experimental low-oxygen PCS-derived fibres
The precursor used was a commercial PCS (from Shin Etsu Co. Ltd, Tokyo, Japan) modified to allow the spinning process.[15] The PCS filaments were cured with an electron beam (EB) under an argon atmosphere (1000 Mrad, 300 Mrad h^{-1}). The irradiated filaments were subsequently pyrolyzed under an argon flow up to 850°C with a heating rate of 50°C h^{-1}. The pyrolysis was then achieved under argon at the final treatment temperature T_p ($1000 < T_p < 1600$°C) for 0·25 h. The fibres are referenced GC1000–GC1600 depending on T_p.

2.1.3 Hi-Nicalon fibre from Nippon Carbon
This recently commercialized fibre is also prepared from the spinning of PCS and subsequent electron beam curing process. They have a very low oxygen content (< 0·5 at%) and are reported to have an excellent thermal stability.[14]

2.1.4 Tyranno Lox-E fibre from UBE
This fibre is probably prepared from the same polymeric precursor as the commercial oxygen-cured Tyranno Lox-M fibre[16,17] namely a polytitanocarbosilane (PTCS) synthesized by mixing polydimethylsilane (PDMS), polyborophenylsiloxane and a tetralkoxide titanate (Ti-$(OR)_4$). Like the Hi-Nicalon fibre, the Tyranno Lox-E (from UBE Industries Ltd, UBE 755, Japan) fibre is prepared by replacing the oxygen curing by an electron beam curing process.[18]

2.1.5 Experimental low-oxygen and low-free carbon fibres from Nippon Carbon
The Hi-Nicalon fibre is almost free of SiO_xC_y phase but still contains a large amount of free carbon (~17 at%) resulting from the starting PCS composition (C/Si (at)~2). For various reasons (e.g. to enhance the oxidation and the creep resistance), several laboratories intended to develop stoichiometric SiC fibres.[12,19–21]

Nippon Carbon has recently developed a new low-oxygen SiC-based fibre derived from PCS but with a near-stoechiometric composition, called 'Hi-Nicalon S' fibre.[19,20] The processing conditions of this fibre are not described in detail in the literature but the innovative step, compared to the standard Hi-Nicalon fibre, might be the pyrolysis conditions rather than the curing process or the polymeric precursor itself For instance, the EB-cured PCS filaments may be pyrolyzed under a hydrogen-rich gas flow to promote the evolution of hydrocarbons from the PCS structure.[21] The organic–mineral transformation would therefore yield a lower free-carbon containing ceramic than the one achieved under an inert atmosphere.

In addition to the Hi-Nicalon fibre (C/Si (at) = 1·41), three experimental samples of low-oxygen SiC based fibres with various free-carbon content (C/Si (at) ranging from 1·38 to 0·91) were provided by Nippon Carbon. The variable free-carbon content is thought to result from the use of different pyrolysis atmosphere conditions (e.g. different hydrogen partial pressures). The fibres are referenced Nicalon(1·38)–Nicalon (0·91) in this paper, depending on the C/Si atomic ratio.

2.2 Thermal annealing
The Hi-Nicalon, Tyranno Lox-E and the experimental low free–carbon fibres were studied in the as-received state but also after heat-treatment in high purity argon at T_p ($1000 < T_p < 1600$°C) during $tp = 1$ h.

2.3 Characterization techniques
Chemical analyses of the bulk of the fibres were performed on polished cross sections by electron probe microanalysis (EPMA) (CAMEBAX 75 from CAMECA) using wave length dispersion spectrometers (PET crystal for Si–K_α and Ti–K_α and PCII multilayer for C–K_α and O–K_α) and pure or stoichiometric standards (respectively SiC, Ti and SiO_2). Hydrogen is not taken into account by EPMA. Elemental analyses were also performed using conventional procedures at the Service Central d'Analyse at CNRS, Vernaison.

The nanostructure of the fibres was investigated by high resolution transmission electron microscopy (TEM) (EM 400 from Philips). The samples

were embedded in epoxy resin, cut into thin foils with an ultramicrotom and set on copper microgrids. The TEM analyses were performed in the bright field (BF), dark field (DF), lattice fringes (LF) and related area diffraction (SAD) modes. Crystalline phases analyses were also carried out by X-ray diffraction (XRD) (D5000 diffractometer from Siemens). The XRD spectra were recorded from tows of fibres. The apparent mean grain size of the SiC crystallites (L) was calculated from the full width at half length (D) of the (111) diffraction peak according to the Scherrer equation: $L = K\lambda/D\cos\theta$ where K is a constant (taken as 1), λ the Cu–K_α wavelength (0·154 nm) and the Bragg angle (17°53′).

Electron spin resonance (ESR) measurements were performed at room temperature with a X-band spectrometer (10^{10} Hz from Varian). The g-value, the line width (S) and the paramagnetic susceptibility (χ_p) were measured. The number of localized paramagnetic centers (η) was determined using DPPH (diphenylpicrylhydrazyle) as a standard.

The electrical conductivity of the fibres (σ) was measured as a function of temperature (T), from room temperature to about −190°C. Two different procedures were used depending on the magnitude of the resistance measured.

For a resistance lower than $10^6\Omega$, a four-points testing device was used. The two ends of a single fibre, whose diameter was previously measured by laser interferometry were glued on a mica plate with an insulating varnish. Four copper wires were then connected to the fibre with silver painting (DAG 1415 from Ackeson). The fibre was submitted to a low electrical current (to avoid a local heating of the fibre by Joule effect) by means of the two outer wires connected to a stable current supply (224 from Keythley) and the two inner wires were then connected to a voltmeter (193 from Keythley). The resistance was calculated in this case from the Ohm law. The main advantage of the four points method is that the measured resistance is not altered by the resistances due to the electrical connections which may be significant.

For a higher magnitude of resistance ($R > 10^6\Omega$) but not exceeding $10^{16}\Omega$, a two-points testing device was used. The resistance was directly measured by means of an electrometer (617 from Keythley). The additional resistances due to the electrical connections are supposed in this case to be negligible compared to that of the fibre. In order to avoid an eventual additional voltage due to a thermoelectric effect of the electrical connections, a second measurement was made after reversing the polarity and the average value of the two measured resistances was considered.

To make low temperature measurements, the testing device consisting of the fibre and its connections on the mica plate was glued at the end of a thermocouple to measure the temperature. The whole system was inserted in a tight glass container filled with helium to facilitate thermal exchanges and to avoid moisture contamination.

The thermal dependence of σ (in $\Omega^{-1}cm^{-1}$) is shown in diagrams where σ is plotted in a logarithmic scale versus the reciprocal temperature ($1000/T$ in K^{-1}). The function $\log\sigma = f(1/T)$ generally obeys a linear variation at least within the temperature range $200 < T < 300$ K and the thermal behaviour of σ can be defined as follows: $\sigma = \sigma_0 \exp(-E_a/k_T)$ where σ_0 is the pre-exponential factor (in $\Omega^{-1}cm^{-1}$), T is the temperature (in K), E_a is the apparent activation energy (in eV) and k is the Boltzmann constant (in eVK^{-1}).

3 Results

3.1 Chemical analysis

The composition of the various SiC-based fibres is shown in Table 1. The chemical concentrations were all measured by EPMA except for the experimental Nicalon(1·38)–Nicalon(0·96) fibres whose composition was provided by Nippon-Carbon. As expected, it clearly appears that the oxygen content of the EB-cured fibres is significantly lower than that of the oxygen-cured fibre (Nicalon NL 200). Except the Nicalon (0·96) fibre, all the fibres contain high amounts of free carbon. The conventional pyrolysis of EB-cured PCS and PTCS filaments (respectively GC1400, Hi-Nicalon and Tyranno Lox-E fibres) generally gives rise to a slightly higher free carbon amount than that of the oxygen-cured PCS fibre (Nicalon NL 200). This feature is probably due to the much lower amounts of carbon atoms engaged in the rare or nearly absent SiO_xC_y phase in the former fibres. The composition of the Hi-Nicalon fibre is close (especially in terms of free carbon) to that of the GC1400 fibre. The higher oxygen concentration of the latter fibre originates from the PCS precursor used which was pre-oxidized in its as-received state.

Table 1. Chemical composition of the different SiC-based fibres (from EPMA, hydrogen is not taken into account)

	Si (at%)	*C (at%)*	*O (at%)*	*Ti (at%)*	*C/Si (at)*	*Free C (at%)*
NL 200	39·5	48·6	12·0	—	1·23	14·9
GC1400	40·0	57·0	3·0	—	1·43	18·5
Hi-Nicalon	41·0	58·0	1·0	—	1·41	17·1
Tyranno Lox-E	36·0	57·0	6·0	0·9	1·58	23·2
Nicalon (0·91)	52·4	47·6	~0	—	0·91	0
Nicalon (1·23)	44·8	55·2	~0	—	1·23	10·4
Nicalon (1·38)	42·0	58·0	~0	—	1·38	16

The Tyranno Lox-E fibre shows low amounts of titanium as well as a relatively high oxygen concentration which both result from the composition of the starting PTCS precursor. The experimental low-free carbon fibres contain significantly lower amounts of free carbon than the standard Hi-Nicalon fibre. The Nicalon(0·96) even shows a silicon excess probably under the form of free silicon. It is worthy of note that the conventional elemental analyses of all the fibres failed in assessing the residual hydrogen concentration. It nevertheless cannot be omitted since the detection limit (0·3 wt%) corresponds to concentration of about 5 at%. Furthermore, a RMN study of pyrolitic residues of PCS showed that the hydrogen concentration can be as high as 4·9 at% (0·27 wt%) for $T_p = 1200°C$ and 0·9 at% (0·03 wt%) for $T_p = 1400°C$.[22,23]

The composition of the fibres (except the Nicalon NL 200 and the low-free carbon fibres) was also measured after thermal annealing in argon up to 1600°C. No significant change in the silicon, titanium, carbon and oxygen concentrations was detected.

Neutron diffraction analysis qualitatively showed the presence of residual hydrogen in the as-received Tyranno Lox-E fibre (it failed for the Hi-Nicalon fibre). The analysis of the fibre after annealing at $T_p = 1400°C$ clearly evidenced the vanishing of hydrogen from the ceramics.[24]

3.2 Structural analyses

The structural properties assessed by TEM analysis of the fibres in the as-processed state and after annealing (the maximal SiC grain size $d(SiC)_{max}$, the extent of the aromatic layer stacks L_a and the number of layers N) are shown in Table 2. The average SiC grain size determined by XRD analysis is shown in Fig. 1.

3.2.1 Experimental PCS-derived fibre (GC fibre)

$T_p = 1000°C$: the microstructure of the fibre is amorphous since no diffraction peak is detected on the XRD spectrum.

Table 2. Structural properties of the different SiC-based fibres (from TEM)

	T_p (°C) $tp\ (h)^{-1}$	$d(SiC)_{max}$ (nm)	L_a (nm)	N
	1200/0·25	6	2–3	4–6
GC fibre	1400/0·25	10	3–5	4–6
	1600/0·25	25	4–8	4–8
	as-received	17	2–3	5–8
Hi-Nicalon	1400/1	25	3–6	5–8
	1600/1	50	5–10	7–12
Tyranno Lox-E	as-received	3–4	1–3	4–5
	1400/1	15	2–4	4–5

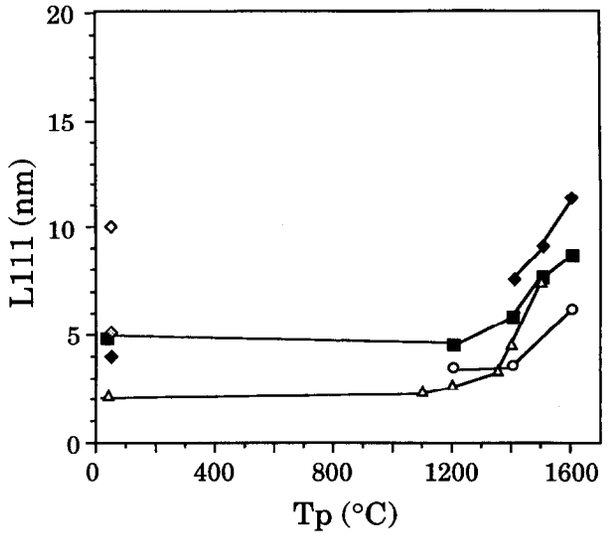

Fig. 1. Apparent average β-SiC grain size (from XRD) of EB-cured polymer-derived fibres, versus the pyrolysis temperature Tp, for tp = 1 h [(○) GC fibre (tp = 0·25h), (■) Hi-Nicalon, (△) Tyranno Lox-E, (◇) Nicalon (0·91), (◆) Nicalon (1·23), (⋄) Nicalon (1·38)].

$T_p = 1200°C$: the SiC_{111} DF imaging of the GC1200 fibre shows very small β-SiC crystallites (2–3 nm) in agreement with the XRD analysis. LF imaging shows free carbon as isolated basic structural units (BSU) (i.e. 2 to 3 layers of about 10 aromatic cycles).

$T_p = 1400°C$: the GC1400 is polycrystalline with a mean apparent SiC grain size of 4 nm (from XRD analysis), a maximum SiC grain size of 10 nm (from SiC_{111} DF) and a free-carbon phase organized as turbostratic stacks of $N = 3$–5 layers partly surrounding SiC crystals. No preferential orientation of either the SiC and the carbon domains is observed.

$T_p = 1600°C$: SiC grains have an apparent mean SiC grain size of 8–10 nm and reach 25 nm as determined by SiC_{111} DF. The extent of the turbostratic stacks (L_a) and the number of layers (N) both increase from $T_p = 1400$ to 1600°C.

3.2.2 Hi-Nicalon fibre

As-received fibre: the nanostructure of the Hi-Nicalon fibre is rather similar to that of the GC1400 fibre. The size of SiC grains currently ranges from 2 to 17 nm with a mean value of about 5 nm. The free carbon domains are $L_a = 2$–3 nm in extent and consist of $N = 5$ to 8 aromatic layers. The turbostratic stacks tend to associate edge to edge flat upon SiC crystals to form an uncompleted intergranular network. LF imaging seldom suggests sintering of SiC crystals.

$T_p = 1400°C$: a SiC grain growth is observed by both XRD and TEM analyses (with a maximum crystal size of 25 nm). Free carbon is also better organized in terms of the extent of the turbostratic

stacks (L_a ranges from 3 to 5 nm). The three-dimensional network of wrinkled carbon domains is more apparent than in the as-received state.

$T_p = 1600°C$: SiC grains as large as 50 nm are observed. Joined SiC crystals are more frequent. The free-carbon phase keeps on organizing with increasing L_a (5–10 nm) and N (7–12) values.

3.2.3 Tyranno Lox-E fibre

As-received: XRD and TEM analyses also show the presence of β-SiC and free carbon phase but in a much lower organization state than that of the Hi-Nicalon fibre. The maximum SiC grain size is 3–4 nm and the carbon domains are slightly thinner (N = 4–5) and significantly shorter (L_a = 1–3 nm).

$T_p = 1400°C$: the SiC grain size increases at $T_p = 1400°C$ with a maximum size of 15 nm but remains lower than the GC1400 fibre or the Hi-Nicalon fibre treated at the same temperature. The free–carbon phase becomes much more organized and apparently abundant. The number of aromatic layers is unchanged (N = 4–5), the extent of the carbon domains is higher (L_a = 2–4 nm) but they remain highly curved.

3.3 Electronic properties

3.3.1 Electron spin resonance

The ESR results are shown in Table 3 for the as-received and heat-treated Hi-Nicalon ($T_p = 1600°C$) and Tyranno Lox-E ($T_p = 1400°C$) fibres. The g-values are similar to these reported for carbon materials (i.e. almost that of the free electron: $g = 0.0023$) and for Nicalon NL 200 fibres.[25] The paramagnetic susceptibility (χ_p) and the linewidth (S) are also close to those reported by other authors for the Nicalon NL 200 fibres.

The g-value is almost unchanged after the heat-treatments while χ_p and the associated spin concentration (η) both strongly decrease for the Hi-Nicalon at $T_p = 1600°C$ (to about one-fifth) and increase for the Tyranno Lox-E at $T_p = 1400°C$ (to the double).

3.3.2 Electrical conductivity

The electrical conductivity of the standard EB-cured fibres (GC1400, Hi-Nicalon and Tyranno Lox-E) is 3 to 4 orders of magnitude higher than that of the oxygen-cured fibre (Nicalon NL 200) (Fig. 2). All the fibres show a typical semi-conducting behaviour (i.e. σ increases with T) which is much more pronounced (the magnitude of E_a is higher) for the Nicalon NL 200 fibre than for the standard EB-cured fibres.

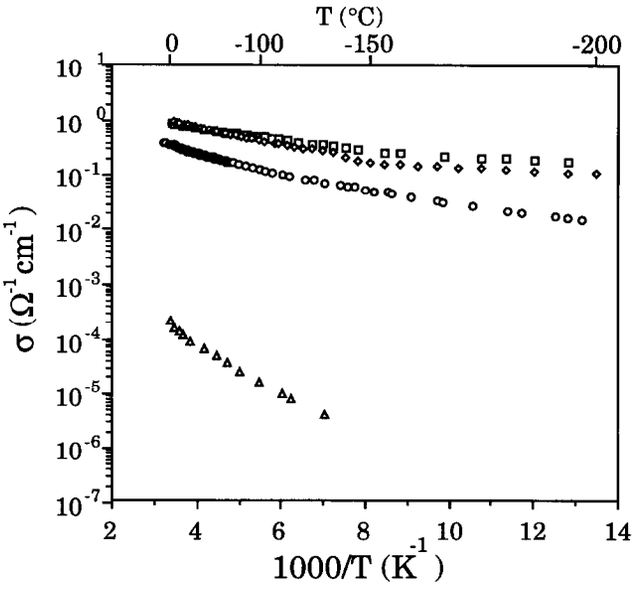

Fig. 2. Thermal behaviour of the electrical conductivity of polymer-derived SiC-based fibres: (□) Hi-Nicalon, (◇) GC1400, (○) Tyranno Lox-E and (△) Nicalon NL200.

The influence of the pyrolysis temperature (T_p) on the electrical conductivity of the PCS-derived EB-cured fibres (GC1000–GC1600) is shown in Fig. 3. The electrical conductivity measured at a given temperature T increases strongly from $T_p = 1000$ to 1200°C (of about 4 decades at 300 K) and then gradually up to $T_p = 1600°C$. For $T_p < 1100°C$, the fibre exhibits a low electrical conductivity ($\sigma < 5{\cdot}10{-}4\ \Omega^{-1}cm^{-1}$) and a marked semi-conducting behaviour ($E_a = 0{\cdot}72$ eV at $T_p = 1000°C$ for $200 < T < 300$ K).

From $T_p = 1100°C$ to 1200°C the d.c. electrical conductivity increases by more than 2 orders of magnitude whereas E_a drops from 0·117 to 0·056 eV. For $T_p \geq 1400°C$, the electrical conductivity becomes almost independent of the temperature. An analysis by Auger electron spectroscopy of the surface of the fibre treated at $T_p = 1600°C$ showed the presence of a thin superficial carbon layer (~350 nm in thickness).[15] In order to study the influence of this carbon layer on the electrical conductivity of the fibre, it was removed by a brief oxidation in air at 600°C. The electrical conductivity of the oxidized fibre is significantly lower

Table 3. ESR results for the different SiC-based fibres

Samples	g	S *(gauss)*	χ_p *(emu CGS g^{-1})*	η *(spin g^{-1})*
Hi-Nicalon as-received/1600°C 1 $h^{-1}Ar^{-1}$	2·0028/2·0027	3·8/2·7	$3{\cdot}30\times10^{-8}/0{\cdot}65\times10^{-8}$	$15{\cdot}5\times10^{18}/3{\cdot}1\times10^{18}$
Tyranno Lox-E as-received/1400°C 1 $h^{-1}Ar^{-1}$	2·0026/2·0027	1·6/1·5	$0{\cdot}28\times10^{-8}/0{\cdot}57\times10^{-8}$	$1{\cdot}3\times10^{18}/2{\cdot}7\times10^{18}$
Nicalon NL200 as-received (26)	2·0027	2·6	—	—

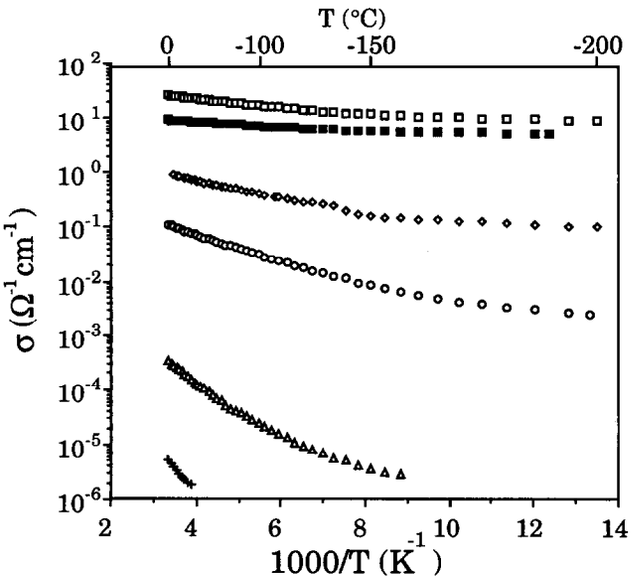

Fig. 3. Thermal behaviour of the electrical conductivity of experimental EB-cured PCS-derived fibres (GC fibers), versus the pyrolysis temperature T_p, for $tp = 1/4$ h [(+) $T_p = 1000$°C, (△) $T_p = 1100$°C, (○) $T_p = 1200$°C, (◇) $T_p = 1400$°C, (□) $T_p = 1600$°C, (■) $T_p = 1600$°C (oxidized 600°C)].

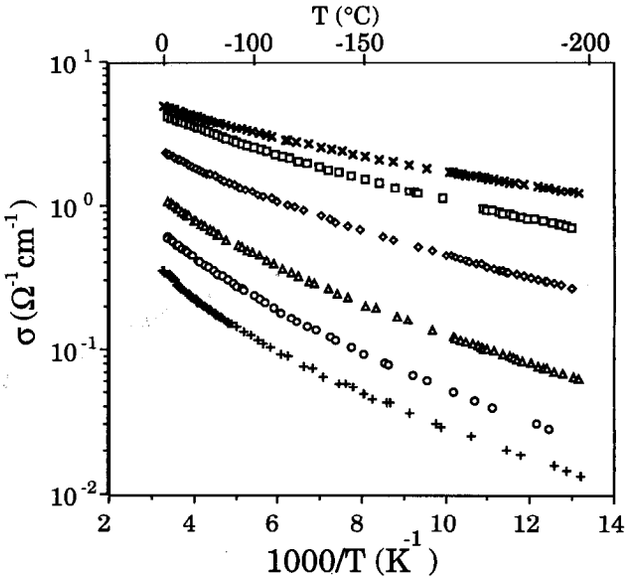

Fig. 5. Thermal behaviour of the electrical conductivity of Tyranno Lox-E fibres, versus the annealing temperature T_p, for $tp = 1$ h [(+) as received, (○) $T_p = 1100$°C, (△) $T_p = 1200$°C, (◇) $T_p = 1300$°C, (□) $T_p = 1350$°C, (X) $T_p = 1400$°C)].

than that of the original fibre but E_a remains almost unchanged.

The influence of the annealing temperature (T_p) on the electrical conductivity of the Hi-Nicalon and Tyranno Lox-E fibres is shown in Figs 4 and 5. As observed above for the experimental ex-PCS EB-cured fibres but to a lower extent, the electrical conductivity of both the Hi-Nicalon at the Tyranno Lox-E fibres increase and the semi-conducting behaviour vanishes (E_a decreases) with T_p. The effect of the thermal treatment is much more pronounced for the Tyranno Lox-E than for the Hi-Nicalon fibre (σ increases of 12 times at $T_p = 1400$°C for the former and only 4 times at $T_p = 1600$°C for the latter) while the electrical conductivity of the Hi-Nicalon is higher than that of the Tyranno Lox-E in the as-received state (respectively 0·8 versus 4·9 $\Omega^{-1}cm^{-1}$). Conversely, the electrical conductivity of the Tyranno Lox-E becomes lower than that of the Hi-Nicalon fibre after annealing at $T_p = 1400$°C (respectively 1·9 versus 4·9 $\Omega^{-1}cm^{-1}$). The influence of the free-carbon content of the experimental EB-cured fibres (Nicalon 1·38–Nicalon 0·91) on their electrical conductivity is shown in Fig. 6. Its room temperature value increases strongly by more than 4 orders of magnitude and the semi conducting behaviour vanishes (E_a decreases) when C/Si ratio is raised from 0·91 to 1·41 (for the Hi-Nicalon fibre). Furthermore, there is a large and sudden evolution of both σ and E_a (σ increases by more than 3 orders of magnitude) from C/Si = 1·23 to 1·38. For C/Si $\leq$ 1·23, the fibres exhibit a remarkably low electrical conductivity ($\sigma < 10^{-4}$ $\Omega^{-1}cm^{-1}$) and a marked semi-conducting behaviour both close to those of the Nicalon NL 200 fibre.

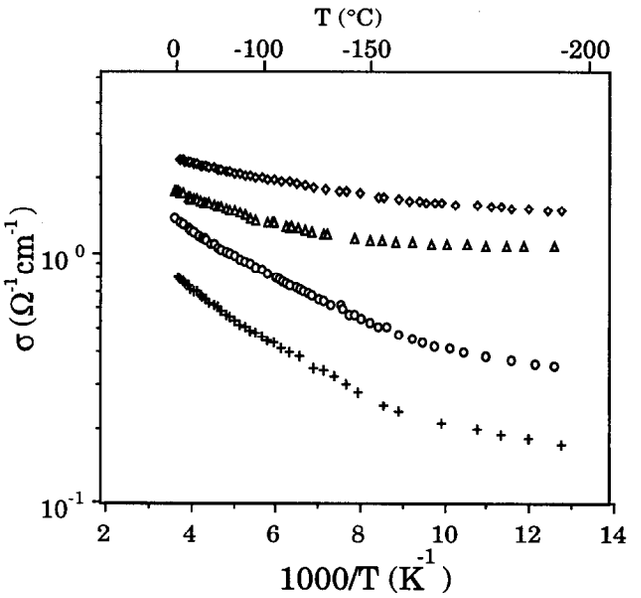

Fig. 4. Thermal behaviour of the electrical conductivity of Hi-Nicalon fibres, versus the annealing temperature T_p, for tp = 1 h ((+) as received, (○) $T_p = 1200$°C, (△) $T_p = 1400$°C, (◇) $T_p = 1600$°C).

4 Discussion

The electrical conductivities at ambient temperature of the EB-cured fibres GC1400, Hi-Nicalon, Tyranno Lox-E and Nicalon (1·38) are all close to 1 $\Omega^{-1}cm^{-1}$ ($0{\cdot}5 < \sigma < 1$ $\Omega^{-1}cm^{-1}$) while those of the oxygen-cured Nicalon NL 200 and of the low-free carbon Nicalon (0·91) and Nicalon (1·23) range

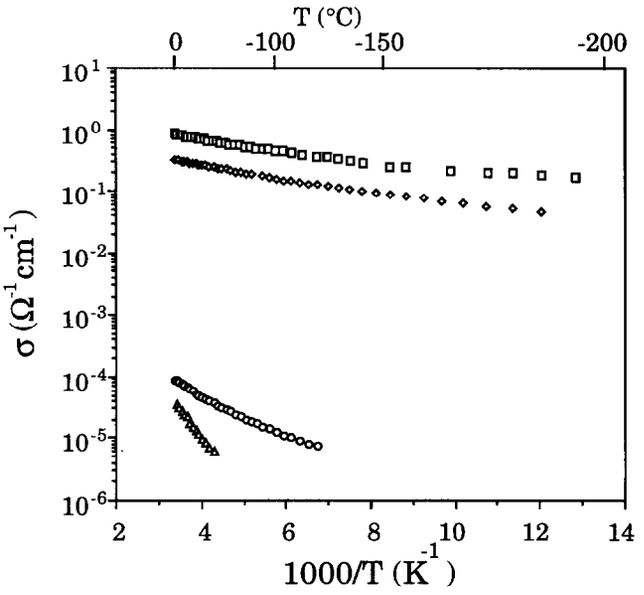

Fig. 6. Thermal behaviour of the electrical conductivity of EB-cured PCS-derived fibres with a varying free carbon content [(△) Nicalon(0·91), (○) Nicalon(1·23), (◇) Nicalon(1·38), (□) Hi-Nicalon(C/Si = 1·41)].

from $5{\cdot}10^{-6}$ to $5{\cdot}10^{-4}$ Ω^{-1}cm^{-1}. Considering that the fibres consist mainly of silicon carbide and free carbon, such a value of σ strongly suggests that the component controlling the electrical behaviour is mainly the free-carbon phase. As a matter of fact, the electrical conductivity of nanocrystallized carbons resulting from the carbonization of anthracene chars currently ranges from 1–100 Ω^{-1}cm^{-1}, depending on the processing temperature.[26–28] As a comparison, σ is only 5–10 Ω^{-1}cm^{-1} for pure polycrystalline CVD SiC. Because of the much lower volume ratio of the free carbon phase to SiC in the former type of fibres (e.g. respectively 14–19 vol% of SiC versus 76 vol% of C in the Hi-Nicalon fibre), such value of σ consistent to that of carbon materials suggests a continuous texture of the free carbon phase throughout the fibre. A simple heterogenous model of the material consisting of a mixture of insulating particles (the SiC grains) and conducting domains (the free carbon) implies a volume ratio of free carbon sufficient to reach the percolation threshold (which is dependent of the shape and the distribution of these domains).[27] Conversely, for lower volume ratios of free carbon [e. g for the Nicalon (0·91) and Nicalon (1·23)], the fibres have such a nanotexture that the carbon phase does not form a continuous network anymore (its volume fraction is below the percolation threshold). The electronic conduction through the fibre cannot be achieved by the free carbon phase only but also partially by the SiC phase. The value of σ is therefore only of the order of that of pure SiC ($5{\cdot}10^{-6}$–$5{\cdot}10^{-4}$ Ω^{-1}cm^{-1}).

The Nicalon NL 200 fibre has a free carbon atomic ratio close to that of the Hi-Nicalon fibre but it exhibits a much lower magnitude of electrical conductivity than its EB-cured counterpart ($2{\cdot}10^{-4} < < 1$ Ω^{-1}cm^{-1}). For a similar reason as described above, this feature might be explained by the discontinuity of the free-carbon phase which would place the Nicalon NL 200 fibre below the percolation threshold. The electrical behaviour would therefore be controlled by the Si–O–C continuum including the SiC grains and the SiO_xC_y oxycarbide phase. As a matter of fact, the free carbon is generally described as isolated BSU's embedded in the Si–O–C continuum.[5] The low value of σ may also be partly related to a low processing temperature yielding a poorly organized and hydrogen-rich free carbon phase characterized by a low electrical conductivity.[27,28] It is worthy of note that TGA analyses have tended to show that the Tyranno Lox-E fibre is not as stable as the Nicalon NL 200 since a weight loss probably due to an evolution of hydrogen was observed for the former fibre at a temperature as low as 1050°C.[24] The Tyranno Lox-E fibre has however a much higher electrical conductivity than that of the Nicalon NL 200. This feature tends to confirm the assumption of the presence of isolated BSU's in the Nicalon NL 200 on one hand and of interconnected carbon domains in the Tyranno Lox-E on the other hand.

All the EB-cured fibres exhibit a semi-conducting type electrical behaviour which gradually vanishes as the electrical conductivity increases, both features as a result of the pyrolysis or annealing temperature T_p increase. Such a behaviour has already been observed for PCS pyrolitic residues [29] and has been described for non-crystalline carbon materials.[27]

A qualitative analysis of the electronic properties of EB-cured fibres during pyrolysis (GC1000–GC1600) can be based on a study of the carbonization of anthracene chars.[27,28] The free-carbon phase of the fibre for T_p > 1000°C can be described by the mixture of two phases; the former is conductive and made of stacked aromatic carbon layers (visible by TEM) long and organized enough to have metal-like electrical properties whereas the latter is insulating, i.e. the faulted carbon (with sp^3 hybridization state), the hydrogenated carbon at the periphery of the aromatic layers and the porosity between the carbon domains. The pyrolysis of the EB-cured fibres results, after the formation of conducting aromatic domains of low extent (T > 850°C),[22] (1) in the elimination of the hydrogen atoms from the periphery of the aromatic layers (and therefore to the formation of free radicals) and (2) in the coalescence of these nano-domains to form larger conducting domains (associated to the decrease of the number of free radicals). From a macroscopic point of view, the coalescence of the

conducting domains beyond the percolation threshold gives rise to a sudden increase of the electrical conductivity (from $T_p = 1100$ to 1200°C), in a similar manner to that for the fibres with variable amounts of free carbon.

A similar behaviour is observed for the Hi-Nicalon and Tyranno Lox-E fibres when submitted to increasing annealing temperatures, but to a lesser extent. As a matter of fact, the fibres were prepared at such high temperatures that the further thermal treatment has only a moderate effect on their microstructure and therefore on their electrical properties. An increase of σ associated with a decrease of E_a is however observed at $T_p = 1100$°C for the Tyranno Lox-E fibre and 1200°C for the Hi-Nicalon fibre, while no structural evolution of the fibres was observed.

The effect of the thermal treatments of both fibres on their concentration of paramagnetic centers (η) is completely different. η increases from the as-received state to $T_p = 1400$°C for the Tyranno Lox-E and decreases at $T_p = 1600$°C for the Hi-Nicalon fibre. These features illustrate the two successive mechanisms described above: (1) an increase of η due to the breaking of C–H bonds at the boundary of the carbon domains and (2) a decrease of N due to the two- dimensional ordering of these domains. The first mechanism is mainly involved for the annealing of the Tyranno Lox-E fibre at $T_p = 1400$°C because of its relatively high concentration of residual hydrogen. It is not necessarily associated with an organization of the free carbon texture, as supported by the TEM analysis which only shows a moderate increase of L_a at $T_p = 1400$°C. Conversely, the second mechanism is mainly involved for the Hi-Nicalon fibre at $T_p = 1600$°C, because of its very low concentration of hydrogen, its significantly better organization of the free carbon phase in the as-received state (also supported by TEM analysis) and finally because of the obvious organization of free carbon observed after annealing at a higher temperature ($T_p = 1600$°C).

5 Conclusion

The electrical properties of various SiC-based fibres prepared from the pyrolysis of organosilicon precursors were studied in correlation with their chemical and structural properties. The magnitude of the electrical conductivity (σ) and its thermal dependence (the apparent activation energy E_a) are mainly controlled by the free-carbon phase present in the fibres.

Free carbon is observed by TEM analysis as turbostratic stacks of aromatic carbon layers. The extent of those carbon domains (in length: L_a and thickness: N) increases with the maximum (post)-processing temperature T_p of the fibres. The amount of free carbon but mainly, its texture, govern the electrical properties of the fibres according to a percolation effect. For instance, isolated carbon domains embedded in an insulating crystalline [Nicalon (0·91) and Nicalon (1·23)] or a partially crystalline (Nicalon NL 200) continuum give rise to an electrical conductivity level which is 4 to 5 orders of magnitude lower than that of fibres with a continuous carbon network (GC1400–GC1600, Hi-Nicalon and Tyranno Lox-E).

For a given amount of free carbon in the material, its organization (i.e. its microstructure and microtexture) significantly influences the magnitude of σ and E_a. The pyrolysis of EB-cured PCS filaments at increasing temperatures results successively (1) in the formation of hydrogenated aromatic domains (GC1000–1100), (2) in the elimination of the hydrogen from the border of the domains (GC1100–GC1400 and Tyranno Lox-E for $T_p = 1400$°C) and (3) in their coalescence into larger conductive domains eventually in the form of a continuous carbon network (GC1400–GC1600, Hi-Nicalon and Tyranno Lox-E for $T_p \geq 1400$°C). From a macroscopic point of view, this phenomenon corresponds to large changes in the d.c. electrical conductivity at room temperature and its temperature dependence.

Acknowledgements

The authors are indebted to Ube Japan for the supply of the Tyranno Lox-E sample and to Nippon Carbon (Japan) for the supply of samples of Hi-Nicalon and experimental low-oxygen and low-free carbon fibres. They gratefully thank F. Laanani and M. Monthioux from the Laboratoire Marcel Mathieu in Pau for the TEM analyses, J. Amiell and A. Marchand from the CRPP in Pessac for conducting ESR experiments and for valuable discussions and M. Czerniak, C. Laporte, B. Aldacourrou and C. Bieler for their assistance in the conductivity measurements.

References

1. Yajima, S., Hayashi, J. and Omori, M., Continuous silicon carbide fibres of high tensile strength. *Chem. Letters*, 1976, **9**, 931–934.
2. Hasegawa, Y., Iimura, M. and Yajima, S., Synthesis of continuous silicon fibres, part 2: Conversion of polycarbosilane fibre into silicon carbide fibres. *J. Mat. Sci*, 1980, **15**, 720–728.
3. Laffon, C., Flanck, A. M., Lagarde, P., Laridjani, M., Hagege, R., Olry, P., Cotteret, J., Dixmier, J., Miquel, J.

L., Hammel, H. and Legrand, A. P., Study of nicalon-based ceramic fibres and powders by EXAFS spectrometry, X-ray diffractometry and some additional methods. *J. Mater. Sci.*, 1989, **24**, 1503–1512.
4. Porte, L. and Sartre, A., Evidence for a silicon oxycarbide phase in the nicalon silicon carbide fibre. *J. Mat. Sci.*, 1989, **24**, 271–275.
5. Le Coustumer, P., Monthioux, M. and Oberlin, A., Understanding nicalon fibre. *J. Eur. Ceram. Soc.*, 1993, **11**, 95–103.
6. Mah, T., Lecht, N., Mc Cullum, D. E., Hoenigman, J. R., Kim, H. M., Katz, A. P. and Lipsitt, H. A., Thermal stability of sic fibres (nicalon). *J. Mater. Sci.*, 1984, **19**, 1191–1201.
7. Johnson, S. M., Brittain, R. D., Lamoreaux, R. H. and Rowcliffe, D. J., Degradation mechanisms of silicon carbide fibres. *J. Am. Ceram. Soc.*, 1988, **71**(3), C132.
8. Jaskowiak, M. H. and Di Carlo, J. A., Pressure effects on the thermal stability of silicon carbide fibres. *J. Am. Ceram. Soc.*, 1989, **72**(2), 192–197.
9. Bender, B. A., Wallace, J. S. and Schrodt, D. J., Effects of thermochemical treatments on the strength and microstructure of sic fibres. *J. Mater. Sci.*, 1991, **26**, 970–971.
10. Toreki, W., Batich, C. D., Sacks, M. D., Saleem, M., Choi, G. J. and Moronne, A. A., Polymer-derived silicon carbide fibres with low-oxygen content and improved thermomechanical stability. *Comp. Sci. Tech.*, 1994, **51**, 146–159.
11. Hasegawa, Y., New curing method for polycarbosilane with unsaturated hydrocarbons and application to thermally stable SiC fibre. *Comp. Sci. Tech.*, 1994, **51**, 161–166.
12. Lipowitz, J., Barnard, T., Bujalski, D., Rabe, J. A., Zank, G. A., Zangvil, A. and Xu, Y., Fine-diameter polycrystalline SiC fibres. *Comp. Sci. Tech.*, 1994, **51**, 167–171.
13. Okamura, K., Matsukawa, T. and Hasegawa, Y., γ-ray irradiation curing on polycarbosilane fibres as the precursor of SiC fibres. *J. Mater. Sci. Letters*, 1985, **4**, 55–57.
14. Takeda, M., Imai, Y., Ichikawa, H., Ichikawa, H., Kasai, N., Segushi, T. and Okamura, K., Thermal stability of the low oxygen silicon carbide fibres derived from polycarbosilane. *Ceram. Eng. Sci. Proc.*, 1992, **13**(7–8), 209–217.
15. Chollon, G., Czerniak, M., Pailler, R., Bourrat, X, Pillot, J. P., Naslain, R. and Cannet, R., A model SiC-based fibre with a low oxygen content prepared from a polycarbosilane precursor. *J. Mat. Sci.*, 1997, **32**, 893–911.
16. Yamamura, T., Ishikawa, T., Shibuya, M., Hisayuki, T. and Okamura, K., Development of a new continuous silicon-titanium-carbon-oxygen fibre using an organometallic polymer precursor. *J. Mat. Sci.*, 1988, **23**, 2589.
17. Ishirkawa, T., Yamamura, T. and Okamura, K., Production mechanism of polytitanocarbosilane and its conversion into inorganic materials. *J. Mat. Sci.*, 1992, **27**, 6627–6634.
18. Yamamura, T., *Tyranno Fibres*, EACM, ECCM-6, Euro-Japanese Colloquium on Ceramic Fibres, ed. A. R. Bunsell and I. Kimpara. Japan Soc. Comp. Mat., Bordeaux, 23–24 Sept. 1993.
19. Ichikawa, H., Okamura, K. and Segushi, T., Oxygen-free ceramic fibre from organosilicon precursors and E-beam curing. In *High Temperature Ceramic Matrix Composites II*, ed. A. G. Evans and R. Naslain. Ceramic Trans. Vol. 58, The American Ceramic Society, Westerville, OH, 1995, pp. 65–74.
20. Narisawa, M., Nakashiba, K. and Okamura, K., Effect of rapid heat treatment on electrical properties of polymer derived ceramic fibers. In *High Temperature Ceramic Matrix Composites II*, ed. A. G. Evans and R. Naslain. Ceramic Trans. Vol. 58, The American Ceramic Society, Westerville, OH, 1995, pp. 287–292.
21. Tazi-Hemida, A., Pailler, R. and Naslain, R., Continuous SiC-based model monofilament with a low free carbon content. Part 1: from the pyrolysis of a polycarbosilane precursor under an atmosphere of hydrogen. *J. Mat. Sci.*, 1997, **32**, 2359–2366.
22. Gerardin, C., Caractérisation par résonance magnétique nucléaire de matériaux céramiques à base de carbure ou carbonitrure de silicium obtenus par voie polymérique, Ph.D. thesis, University of Paris VI, 1991.
23. Gerardin, C., Henry, M. and Taulelle, F., NMR characterization of silicon carbides and carbonitrides. A method for quantifying the silicon sites and the free carbon phase. *Mat. Res. Soc. Symp. Proc.*, ed. M. J. Hampden-Smith, W. G. Klemper and C. J. Brisker, 1992, **271**, 777–782.
24. Chollon, G., Pailler, R., Naslain, R., Laanani, F., Monthioux, M. and Olry, P., Thermal stability of a PCS-derived SiC fibre with a low oxygen content (Hi-Nicalon). *J. Mat. Sci.*, 1997, **32**, 327–347.
25. Chauvet, O., Zuppiroli, L. and Solomon, I., Electronic properties of disordered sic materials. *Mater. Sci. and Eng.*, 1992, **B11**, 303–306.
26. Ricci, M., Carbonitrures hydrogénés obtenus par dépot chimique en phase vapeur assisté par un plasma réactif. Ph.D. thesis, University of Bordeaux, 1991.
27. Delhaes, P. and Carmona, F., Physical properties of non-crystalline carbons. *Chem. Phys. Carbon*, ed. P. A. Thrower, 1981, **17**, 89–174.
28. Carmona, F., Delhaes, P., Keryer, G. and Manceau, J. P., Non-metal transition in a non-crystalline carbon. *Solid State Comm.*, 1974, **14**, 1183–1187.
29. Bouillon, E., Langlais, F., Pailler, R., Naslain, R., Sarthou, J. C., Delpuech, A., Laffon, C., Lagarde, P., Cruege, F., Huong, P. V., Monthioux, M. and Oberlin, A., Conversion mechanisms of polycarbosilane or into SiC-based ceramic material. *J. Mater. Sci*, 1991, **26**, 1333–1345.